Majorana-Based Fermionic Quantum Computation

O'Brien, T. E.; Rożek, P.; Akhmerov, A. R.

DOI
10.1103/PhysRevLett.120.220504

Publication date
2018

Document Version
Final published version

Published in
Physical Review Letters

Majorana-Based Fermionic Quantum Computation

T. E. O'Brien,[1] P. Rożek,[2,3] and A. R. Akhmerov[3]
[1]Instituut-Lorentz, Universiteit Leiden, P.O. Box 9506, 2300 RA Leiden, Netherlands
[2]QuTech, Delft University of Technology, P.O. Box 5046, 2600 GA Delft, Netherlands
[3]Kavli Institute of Nanoscience, Delft University of Technology, P.O. Box 5046, 2600 GA Delft, Netherlands

(Received 13 February 2018; revised manuscript received 5 April 2018; published 1 June 2018)

Because Majorana zero modes store quantum information nonlocally, they are protected from noise, and have been proposed as a building block for a quantum computer. We show how to use the same protection from noise to implement universal fermionic quantum computation. Our architecture requires only two Majorana modes to encode a fermionic quantum degree of freedom, compared to alternative implementations which require a minimum of four Majorana modes for a spin quantum degree of freedom. The fermionic degrees of freedom support both unitary coupled cluster variational quantum eigensolver and quantum phase estimation algorithms, proposed for quantum chemistry simulations. Because we avoid the Jordan-Wigner transformation, our scheme has a lower overhead for implementing both of these algorithms, allowing for simulation of the Trotterized Hubbard Hamiltonian in $\mathcal{O}(1)$ time per unitary step. We finally demonstrate magic state distillation in our fermionic architecture, giving a universal set of topologically protected fermionic quantum gates.

DOI: 10.1103/PhysRevLett.120.220504

Particle exchange statistics is a fundamental quantum property that distinguishes commuting spin or qubit degrees of freedom from anticommuting fermions, despite single particles in both systems only having two quantum states. Different exchange statistics cause a different set of Hamiltonian terms to be local, or even physically possible. For example, although it is Hermitian, the linear superposition of a fermionic creation and annihilation operator $c + c^\dagger$ never occurs as a Hamiltonian term in nature due to violating fermion parity conservation, while spin systems have no such restrictions. Despite these differences, it is possible to simulate fermions using qubits and vice versa [1]. Such simulation necessarily incurs overhead because of the need to transform local fermion operators into nonlocal qubit ones by using, for example, the Jordan-Wigner transformation. Because quantum simulation of the electronic structure of molecules is a promising application of quantum computation [2], much recent work focused on minimizing this overhead of simulating fermionic Hamiltonians with qubits [3–5].

Majorana zero modes (also Majorana modes or just Majoranas) are non-Abelian particles, with two Majoranas combining to form a single fermion (see, e.g., Refs. [6–8] for a review). Spatially separating two Majoranas protects this fermionic degree of freedom, and provides a natural implementation of a topological quantum computer [9,10]. Conservation of fermion parity prevents creating a superposition between the two different parity states of two Majoranas. Therfore, most of the existing proposals combine 4 Majoranas with a fixed fermion parity into a single qubit.

Fermionic quantum computation [1] was so far not actively pursued because of the lack of known ways to protect fermionic degrees of freedom from dephasing. We observe that Majoranas naturally offer this protection, while in addition providing a platform for implementing quantum chemistry algorithms. We therefore show that for the problem of simulating fermionic systems on a Majorana quantum computing architecture, it is both possible and preferable to use fermions composed from pairs of Majoranas instead of further combining pairs of these fermions to form single qubits. Formulating fermionic quantum simulation algorithms in terms of fermions imposes the fermion parity conservation at the hardware level, and prohibits a large class of errors bringing the simulator out of the physical subspace. Furthermore, working natively with fermions, we remove the need for the Jordan-Wigner (or related) transformation to map a fermionic problem to a spin system. When simulating a typical quantum chemistry Hamiltonian, our approach results in a more dense encoding of the computational degrees of freedom. A lower requirement on the amount of needed Majorana states makes our approach a relevant goal for initial experiments that focus on small circuits without error correction. The benefit from using fermionic degrees of freedom becomes more important in simulating local fermionic Hamiltonians, such as the Hubbard model, allowing the simulation of unitary time evolution in $\mathcal{O}(1)$ time per Trotter step, and further reducing the cost of pre-error-correction quantum simulation [11]. Finally, we show how to apply the known magic state distillation protocol in fermionic quantum computation. Combined with the recent realization of the fermionic error correction [12] this provides a fault-tolerant fermionic quantum computer.

Our approach relies on the known set of ingredients to perform universal operations with Majorana states [13]: controllable Josephson junctions, direct Majorana coupling, and Coulomb energy. A possible architecture implementing a Majorana-based fermionic quantum processor is shown in Fig. 1. Because our system cannot be separated into blocks with a fixed fermion parity, the protection of the quantum degrees of freedom is only possible if different parts of the system are connected to a common superconducting ground [14]. Turning off some of the Josephson junctions (these may be either flux-controlled SQUIDs or gate controlled [16,17]) then isolates a part of the system, and generates a Coulomb interaction [18,19],

$$H_C = i^{N/2} E_C \prod_k^N \gamma_k, \tag{1}$$

that couples all the Majorana modes γ_i belonging to the isolated part of the system with the charging energy E_C. An example of such coupling acting on 8 Majorana modes is shown by a red box in Fig. 1. Finally, gate-controlled T junctions exert the interaction

$$H_M = iE_M \gamma_j \gamma_k, \tag{2}$$

on any two Majorana modes coupled by a T junction, with E_M the Majorana coupling energy.

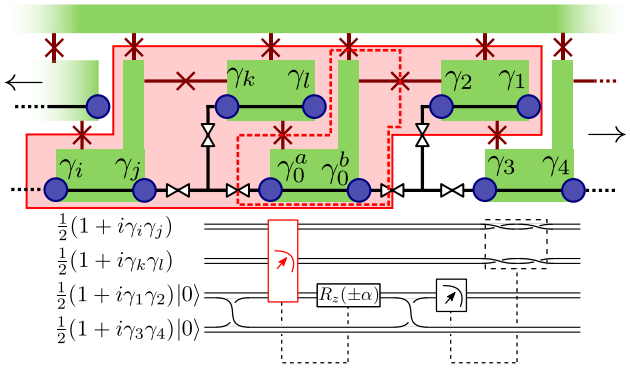

FIG. 1. Top: a 1D implementation of a Majorana circuit. Majoranas (blue dots) occur at either the edge of a nanowire (black line) or as it crosses the boundary of a superconductor (green). Josephson junctions (red crossed lines) connect superconducting islands to a common base, allowing for parallel joint parity measurements. Fully tunable T junctions (valve symbols) allow for a computational Majorana to be shifted from one end of any coupled set of itself and two braiding ancillas (prepared in a known state) to another end. Bottom: an implementation of a weight-four Majorana rotation [Eq. (6)] using the labeled qubits in the design. The operation of individual circuit elements is listed in Table I. The highlighted parity measurement is performed by isolating the highlighted area of the architecture via tunable Josephson junctions, and measuring the total charge parity. This requires a separate preparation of the Majoranas γ_0^a and γ_0^b (dashed red box) in the $i\gamma_0^a\gamma_0^b = 1$ state (which is also required to use these as spare sites for braiding).

Controllable pairwise interactions between Majorana modes [20,21] or two-Majorana parity measurements [22] allow the implementation of braiding, while the joint readout of the fermionic parity of more than 2 Majorana modes generates the rest of the Clifford group [13]. Finally, a diabatic pulse of a two-Majorana coupling implements an unprotected phase gate $e^{\theta\gamma_i\gamma_j}$. We summarize these elementary gates that serve as a basis of our protocol in Table I. This gate set is computationally universal within a fixed fermion parity sector [1].

The above gate set is sufficient to construct circuits for time evolution, quantum phase estimation (QPE), and a variational quantum eigensolver—the unitary coupled cluster ansatz (UCC). Most fermionic systems have Hamiltonians constructed from two- and fourfold fermionic terms:

$$H = \sum_{i,j} h_{i,j} \hat{f}_i^\dagger \hat{f}_j + \sum_{i,j,k,l} \hat{f}_i^\dagger \hat{f}_j^\dagger \hat{f}_k \hat{f}_l. \tag{3}$$

Here, $\hat{f}_i^\dagger$ ($\hat{f}_i$) is the creation (annihilation) operator for an electron. This is equivalent to a sum over two- and fourfold Majorana terms:

$$H = \sum_{i,j} i g_{i,j} \gamma_i \gamma_j + \sum_{i,j,k,l} g_{i,j,k,l} \gamma_i \gamma_j \gamma_k \gamma_l. \tag{4}$$

TABLE I. Basic circuit elements we allow in our computation scheme. The above is sufficient to generate universal quantum computation in the single-parity sector. Computational degrees of freedom are formed by two Majoranas, and are therefore represented as a double line. Preparation, braiding, and measurement gates are assumed to be topologically protected. The $R_z(\theta)$ rotation is not topologically protected, but may be distilled via our magic state distillation protocol. The measurement projects our system onto a state of definite parity $P(b)$, being the sum $\sum_{i,j} \frac{1}{2}(1 + i\gamma_i\gamma_j)$ of the pairs of Majoranas γ_i, γ_j on islands connected to the ground via Josephson junctions.

Name	Element	Operation
Preparation	$i\gamma_1\gamma_2 \ \|0\rangle$	Prepare $\begin{pmatrix} 1 \\ 0 \end{pmatrix}$
Braiding		$\begin{pmatrix} e^{i\pi/4} & 0 \\ 0 & e^{-i\pi/4} \end{pmatrix}$
Braiding		$\begin{pmatrix} 1 & 0 & 0 & -i \\ 0 & 1 & -i & 0 \\ 0 & -i & 1 & 0 \\ -i & 0 & 0 & 1 \end{pmatrix}$
Rotation	$R_z(\theta)$	$\begin{pmatrix} e^{i\theta} & 0 \\ 0 & e^{-i\theta} \end{pmatrix}$
Measurement	m	$\sum_{P(b)=m} \|b\rangle\langle b\|$

Time evolution is performed by applying the Trotter expansion of the evolution operator e^{iHt} [23],

$$e^{iH\Delta t} \underset{\Delta t\to 0}{\approx} \prod_{i,j} e^{-g_{i,j}\gamma_i\gamma_j\Delta t} \prod_{i,j,k,l} e^{ig_{i,j,k,l}\gamma_i\gamma_j\gamma_k\gamma_l\Delta t}, \tag{5}$$

and thus requires consecutive application of the unitary operators $e^{\theta\gamma_i\gamma_j}$ and $e^{i\theta\gamma_i\gamma_j\gamma_k\gamma_l}$. We therefore introduce the weight-$2N$ Majorana rotation operator

$$\exp\left(i\theta\prod_{n=1}^{N} i\gamma_{2n-1}\gamma_{2n}\right), \tag{6}$$

that forms the basis of all the algorithms we consider.

A Majorana rotation may be performed using a generic circuit with an additional four-Majorana ancilla qubit. To demonstrate, the circuit of Fig. 1 applies a Majorana rotation $e^{i\theta\gamma_i\gamma_j\gamma_k\gamma_l}$. The same scheme implements weight-two Majorana rotations by removing Majoranas γ_k and γ_l, and higher weight-$2N$ Majorana rotations by adding $2N-4$ more Majoranas to the correlated parity check and conditional final braiding. The ancillary Majoranas γ_0^a and γ_0^b used for the braiding begin in the parity eigenstate $i\gamma_0^a\gamma_0^b = 1$. The eight-Majorana charge parity measurement $\gamma_i\gamma_j\gamma_k\gamma_l\gamma_0^a\gamma_0^b\gamma_2\gamma_1$ (implemented by isolating the circled superconducting islands in Fig. 1) therefore reduces to the six-Majorana measurement highlighted in the circuit. The unprotected rotation by the angle $\alpha = \theta + (\pi/2)$ both corrects an unwanted phase from the braiding of γ_2 and γ_3, and applies the non-Clifford rotation by θ.

Quantum phase estimation requires the unitary evolution of a state (prepared across a set of system qubits) conditional on a set of ancilla qubits, which then have the eigenphases of the unitary operator encoded upon them [27]. For the purposes of simulating quantum chemistry, a common choice of this operator is the time evolution operator, approximated by the Trotter expansion. In Ref. [28], we show how to encode the ancilla qubit nonlocally across an array of fermions, each of those controlling the unitary evolution of a local Hamiltonian term. This reduces the requirements for QPE to consecutive operations of weight-four and weight-six Majorana rotations, with two Majoranas in each rotation belonging to an ancilla fermion. In Ref. [28] we show how this circuit is used to execute a single Trotter step for a fully connected fourth-order Hamiltonian in $O(N^3)$ time.

Variational quantum eigensolvers prepare a trial state $|\psi(\vec{\theta})\rangle$ from a circuit depending on a set of variational parameters $\vec{\theta}$, which are then tuned to minimize the energy $\langle\psi(\vec{\theta})|H|\psi(\vec{\theta})\rangle$ [29]. One example of such an ansatz is the UCC-2, which uses the exponential of the second order expansion of the cluster operator:

$$|\psi(t_p^r, t_{pq}^{rs})\rangle = e^{T^{(2)}-T^{(2)\dagger}}|\Phi_{\text{ref}}\rangle,$$
$$T^{(2)} = \sum_{p,r} t_p^r \hat{f}_p^\dagger \hat{f}_r + \sum_{p,q,r,s} t_{pq}^{rs} \hat{f}_p^\dagger \hat{f}_q^\dagger \hat{f}_r \hat{f}_s.$$

After Trotterizing, this requires only weight-two or -four Majorana rotations to prepare.

When the Hamiltonian contains a small fraction of all possible second- or fourth-order terms, the lack of Jordan-Wigner strings gives our fermionic architecture an advantage over qubit-based implementations. As an example, we consider the Hubbard model on a square lattice, with Hamiltonian

$$H = -t\sum_{\langle i,j\rangle,\sigma} \hat{f}_{i,\sigma}^\dagger \hat{f}_{j\sigma} + U\sum_i \hat{n}_{i\uparrow}\hat{n}_{i\downarrow} - \mu\sum_{i\sigma}\hat{n}_{i\sigma}. \tag{7}$$

Here σ is a spin index, and the first sum goes over the pairs of nearest neighbor lattice sites, while t, μ, and U are the model parameters [30]. Rewriting the Hubbard model Hamiltonian in terms of Majorana operators $\hat{f}_{i\sigma}^\dagger = \frac{1}{2}(\gamma_{\sigma,1}^i + i\gamma_{\sigma,2}^i)$ gives

$$H = \frac{t}{2}\sum_{\langle i,j\rangle,\sigma} i\gamma_{\sigma,1}^i\gamma_{\sigma,2}^j + N\left(\frac{U}{4}-\mu\right) + \frac{i}{4}(U-2\mu)\sum_{i,\sigma}\gamma_{\sigma,1}^i\gamma_{\sigma,2}^i - \frac{U}{4}\sum_i \gamma_{\uparrow,1}^i\gamma_{\uparrow,2}^i\gamma_{\downarrow,1}^i\gamma_{\downarrow,2}^i. \tag{8}$$

This gives in total 11 terms per site i that need to be simulated for quantum phase estimation or unitary time evolution. In Fig. 2 we show a 2D architecture that

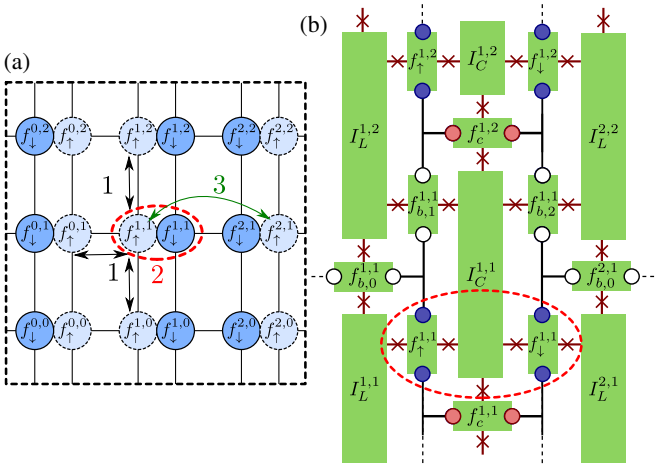

FIG. 2. A 2D Majorana architecture to implement the Hubbard model on a square lattice. (a) A schematic description of the initial layout of the fermions (each of which is made of two Majoranas). Lines denote fermions separated by ancilla Majoranas only. Our scheme groups the 11 Trotter steps into three stages as numbered, which are performed in series. (b) A physical architecture to support the schematic of (a). Wires on superconducting islands and T-junction symbols from Fig. 1 have been removed to prevent cluttering; it is still assumed that all T junctions are fully tunable. Majoranas are colored according to their designation; blue for system fermions, red for control ancillas, and white for braiding and phase ancillas. An example spin-1/2 fermion supported on four Majoranas (the minimum possible) is matched to (a).

implements parallel application of Trotter steps across the entire lattice. For unitary evolution, this scheme is 33% dense, with 12 Majoranas used per site with 2 fermions. For parallel QPE we use an additional ancilla per site (following Ref. [28]), making the scheme 50% dense. We detail the computation scheme for QPE in Ref. [28], achieving a $O(1)$ circuit depth per controlled unitary evolution step. This should be compared first to the $O(N^{1/2})$ circuit depth in the case of a qubit implementation via a parallelized Jordan-Wigner transformation [31]. This circuit depth can be reduced to $O[\log(N)]$ if the Bravyi-Kitaev transformation [1] is used instead, but at the cost of requiring dense qubit connectivity. Separate encodings [32,33] also exist to reduce the circuit depth to $O(1)$, at a cost of doubling the required number of qubits. It is likewise possible to achieve a similar $O(1)$ circuit depth, assuming the ability to couple a global resonator to every qubit in a superconducting architecture [34].

The required ingredient for universal fermionic quantum computation—a Majorana rotation by an arbitrary angle θ—is most simply implemented using an unprotected coupling between two Majoranas. In a scalable architecture this gate needs to have increasingly higher fidelity so that it may be applied an arbitrary number of times without failure. In Fig. 3 we develop a high fidelity Majorana rotation using the magic state distillation protocol of Ref. [35] to perform fermionic gates. In this procedure, we generate 5 low-fidelity $|T\rangle = \cos(\beta)|0\rangle + e^{i\pi/4}\sin(\beta)|1\rangle$ states [$\cos(2\beta) = (1/\sqrt{3})$] on four-Majorana qubits, then combine them to obtain a single higher fidelity $|T\rangle$ state on a qubit (assuming topologically protected Clifford gates). We then use an average of 3 distilled $|T\rangle$ states to perform a $\theta = \pm(\pi/12)$ Majorana rotation. On average, this procedure requires 15 noisy $|T\rangle$ states, 225 braidings, and 66 measurements. We furthermore use 20 Majoranas to make the 5 noisy $|T\rangle$ qubit states, due to the $|T\rangle$ state of a single fermion breaking parity conservation.

The three sources of passive errors in our circuit are fermion parity switches due to nonequilibrium quasiparticles, residual Coulomb coupling in the state where the islands are connected to the ground, and the coupling due to Majorana wave function overlap. These errors also influence other proposals for Majorana-based quantum computation [13]; however, proposals relying on the Coulomb blockade [15,36] are not sensitive to dephasing due the residual Coulomb coupling. The residual Coulomb coupling decays exponentially with the strength of the Josephson junction connecting the superconducting island to the ground [13], and results in dephasing time of $\sim$10 ms for $E_C = E_J/100 = 1$ meV. The coupling due to the Majorana overlap likewise decays exponentially with the spatial separation of Majorana states, reaching $\sim$100 ms for sufficiently large devices [37]. The typical frequency scale of the fermion parity switches depends strongly on the choice of the superconductor, and is currently unknown for Majorana devices.

In summary, we have demonstrated a Majorana-based scheme for fermionic quantum computation. We then adapted this scheme to simulate interacting fermionic Hamiltonians using both the QPE and VQE algorithms, and modified it to simulate the Hubbard model using a constant-depth circuit per time-evolution step. While our fermionic scheme has advantages compared to using qubits, finding optimal circuit layouts for both a general purpose fermionic quantum computation and problem-specific ones, like the Hubbard model simulator, remain an obvious point for further research. Further, our implementation of magic state distillation is a direct translation of

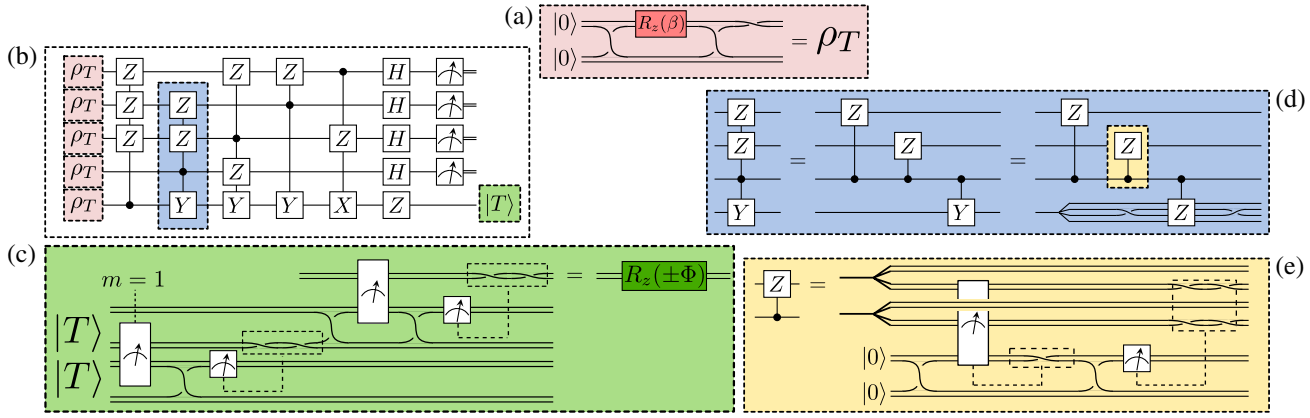

FIG. 3. Circuits for magic state distillation of a non-Clifford fermionic gate, following the scheme of Ref. [35]. (a) A noisy ρ_T state is prepared with a single nontopologically protected gate. (b) 5 such-prepared states are distilled to give a single state with higher fidelity. (c) Two $|T\rangle$ states are consumed to perform a non-Clifford rotation of $\Phi = (\pi/12)$ on a single fermion, restoring universal quantum computation. This requires that the first measurement returns a value of $m = 1$, otherwise a new pair of $|T\rangle$ states must be used. (d) To perform the state distillation protocol, we split the multiqubit conditional gates into two-qubit controlled gates, and then into conditional-Z gates on the underlying fermions by braiding. (e) Controlled Z gate: it may be performed by a circuit requiring braiding and correlated readout with a four-Majorana ancilla.

the original scheme, and it should be possible to find a smaller circuit operating only on fermions, for example, using the minimal fermionic error correcting circuit of Ref. [38]. A final open direction of further research is combining our circuits with quantum error correction [12,38], which would enable fault-tolerant fermionic quantum computation.

We have benefited from discussions with C. W. J. Beenakker, F. Hassler, B. van Heck, M. Wimmer, M. Steudtner, and M. Munk-Nielsen. This research is supported by the Netherlands Organization for Scientific Research (NWO/OCW), as well as ERC Synergy and Starting Grants.

[1] S. B. Bravyi and A. Y. Kitaev, Fermionic quantum computation, Ann. Phys. (Amsterdam) **298**, 210 (2002).
[2] M. Reiher, N. Wiebe, K. M. Svore, D. Wecker, and M. Troyer, Elucidating reaction mechanisms on quantum computers, Proc. Natl. Acad. Sci. U.S.A. **114**, 7555 (2017).
[3] M. B. Hastings, D. Wecker, B. Bauer, and M. Troyer, Improving quantum algorithms for quantum chemistry, Quantum Inf. Comput. **15**, 1 (2015).
[4] I. Kivlichan, J. McClean, N. Wiebe, C. Gidney, A. Aspuru-Guzik, G.-L. Chan, and N. Babbush, Quantum Simulation of Electronic Structure with Linear Depth and Connectivity, Phys. Rev. Lett. **120**, 110501 (2018).
[5] R. Babbush, N. Wiebe, J. McClean, J. McClain, H. Neven, and G.-L. Chan, Low-Depth Quantum Simulation of Materials, Phys. Rev. X **8**, 011044 (2018).
[6] J. Alicea, New directions in the pursuit of Majorana fermions in solid state systems, Rep. Prog. Phys. **75**, 076501 (2012).
[7] C. Beenakker, Search for Majorana fermions in superconductors, Annu. Rev. Condens. Matter Phys. **4**, 113 (2013).
[8] M. Leijnse and K. Flensberg, Introduction to topological superconductivity and Majorana fermions, Semicond. Sci. Technol. **27**, 124003 (2012).
[9] A. Y. Kitaev, Unpaired Majorana fermions in quantum wires, Phys. Usp. **44**, 131 (2001).
[10] S. D. Sarma, M. Freedman, and C. Nayak, Majorana zero modes and topological quantum computation, Quantum Inf. Comput. **1**, 15001 (2015).
[11] P.-L. Dallaire-Demers and F. K. Wilhelm, Method to efficiently simulate the thermodynamic properties of the Fermi-Hubbard model on a quantum computer, Phys. Rev. A **93**, 032303 (2016).
[12] Y. Li, Fault-tolerant fermionic quantum computation based on color code, arXiv:1709.06245.
[13] T. Hyart, B. van Heck, I. C. Fulga, M. Burrello, A. R. Akhmerov, and C. W. J. Beenakker, Flux-controlled quantum computation with Majorana fermions, Phys. Rev. B **88**, 035121 (2013).
[14] The need to use a common superconducting ground makes it impossible to utilize the partial protection from quasiparticle poisoning by applying Coulomb blockade to superconducting islands containing individual qubits [15].
[15] T. Karzig, Christina Knapp, R. M. Lutchyn, P. Bonderson, M. B. Hastings, C. Nayak, J. Alicea, K. Flensberg, S. Plugge, Y. Oreg, C. M. Marcus, and M. H. Freedman, Scalable designs for quasiparticle-poisoning-protected topological quantum computation with Majorana zero modes, Phys. Rev. B **95**, 235305 (2017).
[16] T. W. Larsen, K. D. Petersson, F. Kuemmeth, T. S. Jespersen, P. Krogstrup, J. Nygård, and C. M. Marcus, Semiconductor-Nanowire-Based Superconducting Qubit, Phys. Rev. Lett. **115**, 127001 (2015).
[17] G. de Lange, B. van Heck, A. Bruno, D. J. van Woerkom, A. Geresdi, S. R. Plissard, E. P. A. M. Bakkers, A. R. Akhmerov, and L. DiCarlo, Realization of Microwave Quantum Circuits Using Hybrid Superconducting-Semiconducting Nanowire Josephson Elements, Phys. Rev. Lett. **115**, 127002 (2015).
[18] L. Fu, Electron Teleportation via Majorana Bound States in a Mesoscopic Superconductor, Phys. Rev. Lett. **104**, 056402 (2010).
[19] B. van Heck, F. Hassler, A. R. Akhmerov, and C. W. J. Beenakker, Coulomb stability of the 4π-periodic Josephson effect of Majorana fermions, Phys. Rev. B **84**, 180502 (2011).
[20] J. D. Sau, D. J. Clarke, and S. Tewari, Controlling non-Abelian statistics of Majorana fermions in semiconductor nanowires, Phys. Rev. B **84**, 094505 (2011).
[21] B. van Heck, A. R. Akhmerov, F. Hassler, M. Burrello, and C. W. J. Beenakker, Coulomb-assisted braiding of Majorana fermions in a Josephson junction array, New J. Phys. **14**, 035019 (2012).
[22] C. Knapp, M. Zaletel, D. E. Liu, M. Cheng, P. Bonderson, and C. Nayak, The Nature and Correction of Diabatic Errors in Anyon Braiding, Phys. Rev. X **6**, 041003 (2016).
[23] We have not discussed post-Trotter methods such as Refs. [24–26] in this work. However, these methods still require the Jordan-Wigner transformation or equivalent to represent a fermionic Hamiltonian on a qubit architecture. As such, they gain a similar advantage to the studied Trotterized evolution of e^{iHt} from a Majorana-based fermion implementation.
[24] D. Berry and A. Childs, Black-box Hamiltonian simulation and unitary implementation, Quantum Inf. Comput. **12**, 29 (2012).
[25] D. Berry, M. Kieferová, A. Scherer, Y. R. Sanders, G. H. Low, N. Wiebe, C. Gidney, and R. Babbush, Improved techniques for preparing eigenstates of fermionic Hamiltonians, Quantum Inf. Comput. **4**, 22 (2018).
[26] D. Poulin, A. Kitaev, D. S. Steiger, M. B. Hastings, and M. Troyer, Fast Quantum Algorithm for Spectral Properties, arXiv:1711.11025.
[27] A. Yu. Kitaev, Quantum measurements and the Abelian Stabilizer Problem, arXiv:quant-ph/9511026.
[28] See Supplemental Material at http://link.aps.org/supplemental/10.1103/PhysRevLett.120.220504 for details of algorithms used in the text.
[29] A. Peruzzo, J. McClean, P. Shadbolt, M.-H. Yung, X.-Q. Zhou, P. J. Love, A. Aspuru-Guzik, and J. L. O'Brien, A variational eigenvalue solver on a photonic quantum processor, Nat. Commun. **5**, 4213 (2014).

[30] H. Tasaki, The Hubbard model - an introduction and selected rigorous results, J. Phys. Condens. Matter **10**, 4353 (1998).

[31] Z. Jiang, K. J. Sung, K. Kechedzhi, V. N. Smelyanskiy, and S. Boixo, Quantum Algorithms to Simulate Many-Body Physics of Correlated Fermions, Phys. Rev. Applied **9**, 044036 (2018).

[32] V. Havlíček, M. Troyer, and J. D. Whitfield, Operator locality in the quantum simulation of fermionic models, Phys. Rev. A **95**, 032332 (2017).

[33] J. D. Whitfield, V. Havlíček, and M. Troyer, Local spin operators for fermion simulations, Phys. Rev. A **94**, 030301 (2016).

[34] G. Zhu and Y. Subaşı, J. Whitfield, and M. Hafezi, Hardware-efficient fermionic simulation with a cavity–QED system, Quantum Inf. Comput. **4**, 16 (2018).

[35] S. Bravyi and A. Kitaev, Universal quantum computation with ideal Clifford gates and noisy ancillas, Phys. Rev. A **71**, 022316 (2005).

[36] S. Plugge, A. Rasmussen, R. Egger, and K. Flensberg, Majorana box qubits, New J. Phys. **19**, 012001 (2017).

[37] C. Knapp, T. Karzig, R. M. Lutchyn, and C. Nayak, Dephasing of Majorana-based qubits, Phys. Rev. B **97**, 125404 (2018).

[38] S. Vijay and L. Fu, Quantum Error Correction for Complex and Majorana Fermion Qubits, arXiv:1703.00459.